6th International Conference on Advances in Experimental Structural Engineering
11th International Workshop on Advanced Smart Materials and Smart Structures Technology
August 1-2, 2015, University of Illinois, Urbana-Champaign, United States

Bridge Natural Frequency Estimation by Extracting the Common Vibration Component From the Responses of Two Vehicles

T. Nagayama [1], A. P. Reksowardojo[2], D. Su [2], T. Mizutani [2] C. Zhang [2]

1 *Associate professor, Dept. of Civil Engineering, the University of Tokyo, Japan.*
E-mail: nagayama@bridge.t.u-tokyo.ac.jp
2. *Dept. of Civil Engineering, the University of Tokyo, Japan.*

ABSTRACT
While bridge natural frequencies are among fundamental properties of bridges, natural frequencies of most bridges remain unknown. Natural frequency identification through acceleration measurement with sensors installed on bridges is not practical if a large number of bridges are investigated. Indirect methods to detect the frequencies from the acceleration responses of a vehicle driving over bridges, on the other hand, still have difficulties. Vehicle responses contains various components, making it difficult to distinguish the bridge frequency from other frequency components. This study proposes new frequency estimation strategy utilizing two vehicles. The key idea is that bridge vibration, a common vibration component among responses of multiple vehicles, is extracted through signal processing involving cross-spectrum estimation. Numerical analyses employing a vehicle-bridge interaction (VBI) model are conducted to examine the algorithm performance under various conditions. The numerical simulations have confirmed the feasibility of such indirect frequency detection. An experimental study featuring synchronized-sensing of two vehicles is then performed. The first natural frequency of the bridge has been identified under various driving speed combinations, demonstrating the performance of the proposed approach.

KEYWORDS: *vehicle-bridge identification system, indirect frequency estimation, bridge frequency estimation, bridge assessment*

1. INTRODUCTION

While bridge natural frequencies are among fundamental properties of bridges, natural frequencies of most bridges remain unknown. Natural frequencies, considered to reflect bearing conditions and characterize resonance phenomena under periodic loading, are typically identified through acceleration measurement with sensors installed on bridges [1]. Nonetheless, sensor installation on a large number of bridges is not practical. Installation of instruments to the structure involves a costly process and often encounters site-specific technical difficulties.

Indirect methods to detect the frequencies from the acceleration responses of a vehicle driving over bridges have been studied [2,3,4]. Vehicle-based measurement centers on the concept that bridge vibration influences the vehicle response as a result of vehicle-bridge interaction (VBI) process. Therefore, it is theoretically feasible to obtain bridge natural frequency from the frequency spectrum of the vehicle response. The feasibility has been verified in several studies by means of closed-form solution [2, 4], finite element simulations [2, 3, 4, 5] and experiments [2, 6, 7]. In practice, however, application of vehicle-based measurement is difficult. Typically, the spectral peak associated with bridge frequency is low in magnitude. In some cases, road roughness components are prevalent [3, 5] to the extent that road roughness components nullify the bridge related frequency peak. Identification of bridge natural frequencies among a large number of frequency peaks without a priori knowledge of the bridge frequencies is challenging.

This study proposes new frequency estimation strategy utilizing two vehicles. Bridge vibration, a common vibration component among responses of multiple vehicles, is extracted through signal processing. Signal processing techniques investigated include cross spectrum estimation, spectrum averaging and envelop technique, and frequency domain decomposition [8]. In this paper, bridge natural frequency identification using the cross spectrum estimation, which is shown to be most effective among the three in extracting the bridge vibration components, is proposed. Numerical analyses employing a vehicle-bridge interaction (VBI) model are conducted to examine the algorithm performance under various conditions. The numerical simulations have confirmed the feasibility of such indirect frequency detection. An experimental study featuring

synchronized-sensing of two vehicles is then performed. The vehicles are of different types, leaving the bridge frequency as the remaining signal commonality. The first natural frequency of the bridge has been identified under various driving speed combinations, demonstrating the natural frequency identification performance of the proposed approach

2. EXTRACTION OF BRIDGE NATURAL FREQUENCY USING CROSS-SPECTRUM

Vibrations of a vehicle on a bridge has two main excitation sources (i.e., bridge vibration and road roughness). The spectra of the responses of two vehicles potentially contain common frequency components from these two sources. While vehicle responses associated to the road roughness can be large depending on the road profile, their frequency peaks are not necessarily sharp due to the random nature of road roughness. In terms of commonality of two signals, the vehicle response components due to road roughness are not perfectly common because of variation in running trajectories and driving speeds. On the other hand, bridge vibration components are typically not as large as the components due to road roughness. In terms of signal commonality, the bridge vibration components are considered approximately common to multiple vehicles on the same bridge; in particular, first vertical mode vibration, where all locations of the bridge vibrate in phase, is considered to commonly appear on all vehicles on the bridge though local difference in mode shape amplitude affects signals. The bridge vibration components, approximately common to multiple vehicles, are extracted through cross-spectrum estimation [9]:

$$G_{xy}(f) = \lim_{T\to\infty} \frac{2}{T} E[X^*(f)Y(f)] \tag{2.1}$$

where E [·] denotes the expectation operator and * denotes complex conjugate.

The bridge frequency estimation process with cross-spectrum is summarized as follows:
1) Vibration data of two vehicles, A and B, are collected when two vehicles are on the same bridge (Figure 2.1).
2) Power spectral density of each signal, as well as cross-spectrum of both signals, are computed.
3) Prominent peaks of the cross-spectrum are identified. The prominence of a peak is quantified by the clarity index, with the following formulation:

$$I_i = \frac{G(f_i)}{\frac{1}{n}\sum_{f=f_l}^{f_u} G(f_i)} \tag{2.2}$$

where f_i is the frequency of the peak, f_l and f_u are the lower- and upper-frequency limits of the frequency range of interest. These limits are set as 0 and 10 Hz, respectively, considering possible bridge natural frequency range in this study. Peak *i* is considered as prominent when its associated clarity index I_i is greater than 3.
4) The differences between clarity index I_i and corresponding clarity indices of power spectrum $I_{i,A}$ and $I_{i,B}$, ΔI_i, are computed as $\Delta I_{i,A} = I_i - I_{i,A}$ and $\Delta I_{i,B} = I_i - I_{i,B}$.
5) A prominent peak with the largest value of $\Delta I_{i,A}$and $\Delta I_{i,B}$ is a frequency component with substantial commonality and identified as a bridge natural frequency estimate.

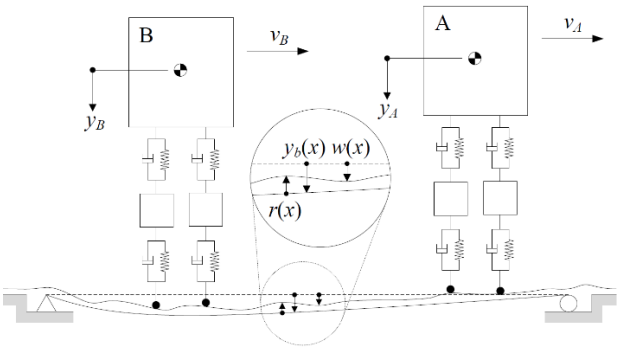

Figure 2.1 The numerical model of two vehicles on a bridge

3. NUMERICAL FEASIBILITY STUDY

3.1. Vehicle-Bridge Interaction (VBI) Formulation

Several Vehicle-bridge interaction (VBI) system models have been developed. Efficiency in terms of computational resource usage, nonetheless, varies. Element-level coupling method, as pointed out by Yang et al. [10] has the best performance. The method consists of multiple equations of motion:

$$[M_v]\{\ddot{u}_v\} + [C_v]\{\dot{u}_v\} + [K_v]\{u_v\} = \{F_{cv}\} \quad (3.1)$$
$$[M_{b,i}]\{\ddot{u}_{b,i}\} + [C_{b,i}]\{\dot{u}_{b,i}\} + [K_{b,i}]\{u_{b,i}\} = \{F_{cb,i}\} \quad (3.2)$$

Eq. 3.1 and Eq. 3.2 represent the equation of motions associated to vehicle and bridge, respectively. Note that the index *i* denotes the bridge element corresponding to the vehicle location. Simulation of *n* vehicles can be achieved simply by employing Eq. 3.1 *n* times. Encapsulated in the interaction load term of vehicle $\{F_{cv}\}$ is the road profile, which is computed using a pre-described power spectral density with trigonometric sum technique [11]:

$$r(x) = \sum_{i=1}^{N} A_i \left(\sin \Omega_i x - \phi_i\right) \quad (3.3)$$

where ϕ_i is uniformly distributed random phase angles U (0,2p), A_i is $\sqrt{\Phi(\Omega_i)\Delta\Omega\pi^{-1}}$ and $\Delta\Omega$ is the frequency sampling rate of the power spectral density. Note that Ω denotes angular spatial frequency.

As shown in Figure 3.1 a 4-DOF model of vehicle, which represents vertical and rotational movement of the body, as well as vertical movement of the axles, is employed. The subsystem matrices of a 4-DOF model and the response vector u_v are as follows:

$$[M_v] = \begin{bmatrix} m_v & & & \\ & j_v & & \\ & & m_1 & \\ & & & m_2 \end{bmatrix} \quad (3.4)$$

$$[C_v] = \begin{bmatrix} c_1 + c_2 & c_2b_2 - c_1b_1 & -c_1 & -c_2 \\ c_2b_2 - c_1b_1 & c_1{b_1}^2 - c_2{b_2}^2 & c_1b_1 & -c_2b_2 \\ -c_1 & c_1b_1 & m_1 & 0 \\ -c_2 & -c_2b_2 & 0 & m_2 \end{bmatrix} \quad (3.5)$$

$$[K_v] = \begin{bmatrix} k_1 + k_2 & k_2b_2 - k_1b_1 & -k_1 & -k_2 \\ k_2b_2 - k_1b_1 & k_1{b_1}^2 - k_2{b_2}^2 & k_1b_1 & -k_2b_2 \\ -k_1 & k_1b_1 & k_1 + k_{t1} & 0 \\ -k_2 & -k_2b_2 & 0 & k_1 + k_{t2} \end{bmatrix} \quad (3.6)$$

$$\{u_v\} = [y \quad \theta \quad y_1 \quad y_2]' \quad (3.7)$$

The bridge is modelled as a simple beam with the length of *L*, a uniform flexural rigidity of *EI* and a mass per unit length of $\overline{m}$. Rayleigh damping is employed. The bridge is modeled with 6-DOF beam elements.

By employing the Newmark-β method, the assembled system of vehicle and bridge in tandem is solved to obtain the vehicle and bridge responses. For unconditional stability, parameters β and γ of the Newmark-β method are selected as 0.25 and 0.5.

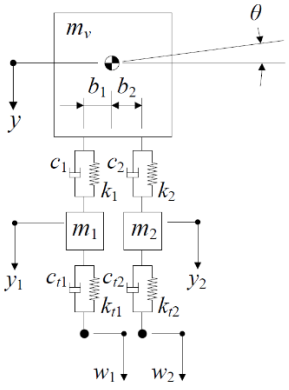

Figure 3.1 vehicle model

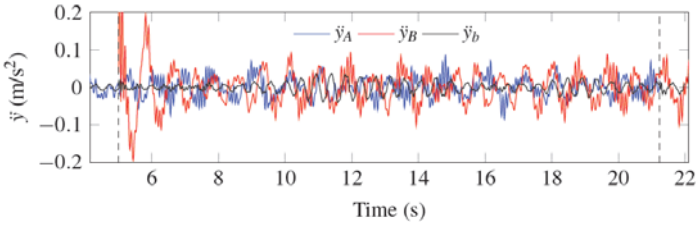

Figure 3.2 Simulated vertical acceleration of vehicles and bridge midspan

3.2. Numerical Results

Simulated vertical accelerations of two vehicles successively passing a bridge with 30 km/h driving speed are shown in Figure 3.2. The dashed lines in the figure indicate the starting and ending point of data included in spectral analysis. During this period between the start and end points, both vehicles are over the bridge. Physical parameters of the vehicles are adopted with modifications from McGetrick et al. [3]. Those parameters are: $m_v = 16600\ kg,\ j_v = 64598\ kg \cdot m^2, m_i = 700\ kg, c_i = 10 \times 10^3\ Ns/m, k_i = 4 \times 10^5 N/m$ and $k_{ti} = 3.5 \times 10^6\ N/m$. The frequencies of pitching and bouncing modes are 0.995 Hz and 1.046 Hz respectively. The parameters of vehicle A and vehicle B are differed by treating those of vehicle A as the reference values while scaling those of vehicle B with a multiplier. As for the bridge, its physical parameters are: $EI = 1.06 \times 10^5 MN \cdot m^2$ and $\overline{m} = 4406.78\ kg/m$. Road profile is generated according to the power spectral density of Class A surface provided in ISO8608 [12].

Figure 3.3a shows the individual power spectra computed from the responses of vehicle A and B. For the sake of brevity, individual power spectra are simply referred to as PSD A and PSD B hereafter. The dashed vertical line indicates $f_{b,1}$ = 2:21 Hz, the bridge natural frequency calculated through eigenvalue analysis, a value that is supposedly unknown in the real measurement. At this stage, it is not possible to identify a peak which is a bridge natural frequency without a priori knowledge of the value. A dominant peak is noticeable in the PSD A within the proximity of vehicle frequency. In PSD B several dominant peaks are visible not only in the region of vehicle frequency, but also in the region near the bridge natural frequency.

In the cross-spectrum in Figure 3.3b, four peaks are prominent. By following the aforementioned procedure, the relative change of clarity indices for all prominent peaks between those of cross-spectrum and individual spectra (PSD A and PSD B) are computed. Table 3.1 presents $\Delta I_{i,A}$ and $\Delta I_{i,B}$. Peak 4 at 2.18 Hz exhibits the largest increase in clarity index, which is strong indication of frequency commonality.

As for the higher modal frequencies ($f_{b,2}$, $f_{b,3}$,…), their peaks are unidentifiable in the individual power spectra as well as in the cross-spectrum. Only the first mode of the beam is significantly excited [10, 13, 14].

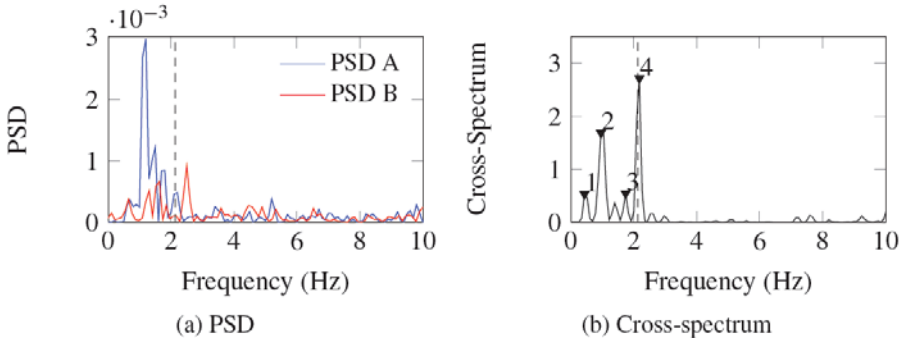

Figure 3.3 PSDs and Cross-spectrum from simulation

Table 3.1 Clarity index changes ΔI_i obtained from simulation

i	1	2	3	4
f_i(Hz)	0.44	0.96	1.74	2.18
$\Delta I_{i,A}$	3.93	5.70	-0.11	17.94
$\Delta I_{i,B}$	4.01	12.30	0.76	16.60
Σ	7.94	18.00	0.65	34.54●

The numerical simulation is performed under different conditions (i.e., drive speed and spacing between the vehicles). The influence of driving speed within the range of v = [5,80] km/h, in conjunction with the influence of inter-vehicle spacing within the range of b = [1,10] m are investigated. Drive speed of vehicle B is set 10 % smaller than that of vehicle A so that the vibration components due to road profile of a certain wave length appear at different frequencies for the two vehicles. Figure 3.4 presents feasible region of measurement (FRM), that is the conditions where identification of bridge natural frequency peak is possible. In FRM, the bridge

natural frequency have the largest value of $\Delta I_{i,A} + \Delta I_{i,B}$ among prominent peaks. The FRM of the identification using either PSD A or PSD B are conditions where bridge natural frequency peak happens to have the greatest amplitude in the spectrum. The FRM of cross spectrum approach is substantially larger than those of PSD A and PSD B. With too large speed, it is not possible to identify the bridge natural frequency because only short acceleration data are obtained; the resulting spectra are poor in frequency resolution.

Vehicle-driven resonance takes place when certain conditions of driving speed and inter-vehicles spacing are met [10]. Large vibration levels under this resonance are considered advantageous for the frequency identification. The resonance condition is reviewed herein.
The frequency of vehicle passage, driving frequency, is written using the reciprocal of vehicle passage duration with the assumption of a constant velocity of v and a bridge span length of L:

$$\alpha = \frac{v}{2L} \tag{3.8}$$

The existence of this frequency implies the occurrence of dynamic resonance in cases where driving frequency or its multiple coincides with the bridge natural frequencies. A non-dimensional parameter is introduced:

$$S_n = \frac{n\alpha}{f_{b,n}} = \frac{nv}{2f_{b,n}L} \tag{3.9}$$

where $f_{b,n}$ is the n-th bridge natural frequency. A sequence that consists of several vehicles travelling at identical constant velocity of v with the spacing of b generates spacing-related frequency as follows:

$$\lambda = \frac{v}{b} \tag{3.10}$$

This spacing frequency also give rise to dynamic resonance in cases where spacing frequency or its multiple coincides with the bridge natural frequencies. A non-dimensional parameter of R_n is introduced.

$$R_n = \frac{\lambda}{f_{b,n}} = \frac{v}{f_{b,n}b} \tag{3.11}$$

For simplicity, only the first bridge natural frequency is discussed. Suppose that the resonance occurs whenever the first bridge natural frequency $f_{b,1}$ coincides with the spacing frequency λ or its multiple. As R_1 is integer k,

$$b = \frac{kv}{f_{b,1}} \tag{3.12}$$

Then by substituting S_1 from Eq. 3.9 into the expression above:

$$b = 2kS_1L \tag{3.13}$$

This resonance criteria of $k = \{1,2,3,4\}$ is superposed on Figure 3.4. The criterion implies that the longer the bridge is, the lower the driving speed is for the resonance to occur when the vehicle spacing is the same. Furthermore, FRMs appear to cluster around the resonance criteria.

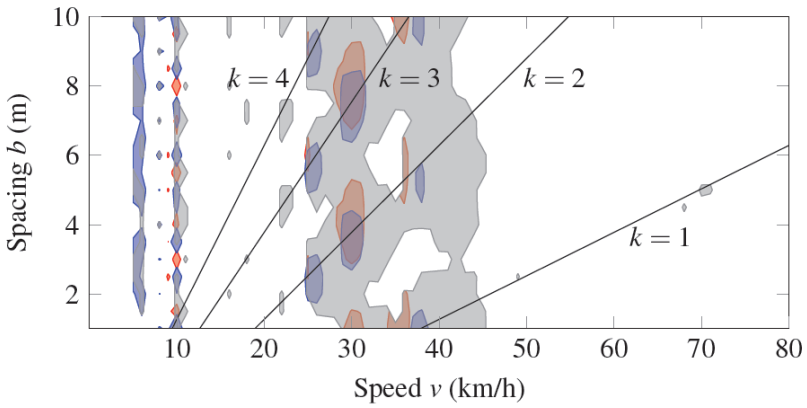

Figure 3.4 Feasible region of measurement: (■) PSD A, (■) PSD B and (■) Cross-spectrum

4. EXPERIMENTAL STUDY

An experimental study has been conducted at a 59-m simply supported steel box-girder bridge. The target bridge, Tsukige Bridge, is located in Kimitsu City, Chiba Prefecture, Japan. The width of the bridge is 4 m, accommodating only one drive lane. Figure 4.1 illustrates the measurement vehicles and equipment. Two light commercial vehicles employed in the experiment are Toyota Land Cruiser and Toyota Hiace van for Vehicle A and Vehicle B, respectively. High accuracy MEMS-type triaxial accelerometers [15] are installed on the two vehicles. The first natural frequencies of these vehicle are identified as 1.46Hz and 1.62 Hz, respectively, through free-vibration tests though large vehicle damping prevented their accurate estimation. An additional accelerometer is attached directly on the bridge surface to obtain the bridge natural frequencies for reference. These frequencies are identified as 2.17 Hz and 5.43 Hz for the 1th and 2nd mode, respectively. Sampling rates of the accelerometers are all set at 1 kHz. The test was repeated four times with different target drive speed combinations shown in Table 4.1.

PC-driven data acquisition systems are connected with GPS receivers. By triggering the data acquisition periodically using the GPS pulse signal, the data acquisition features 30 ns time synchronization accuracy. GPS receiver also acquires UTC clock time and appends the timestamp to acceleration records. In conjunction with timestamping, GPS receiver captures velocity. Both timestamping and velocity acquisition are performed at 1 Hz.

Figure 4.2 presents power spectra and a cross-spectrum of the vehicle responses. Table 4.2 presents the corresponding clarity indices I_i. Peak 4 at 2.17 Hz exhibits the largest increase in clarity index. For each drive speed case, the vehicles run over the bridge ten times. Though keeping constant drive speeds over the bridge is not trivial, a stable drive speed is achieved in most cases according to the GPS record. The bridge natural frequency is identified in most cases as shown in Figure 4.3.

One should direct their attention, however, to the result of Case 4 (Figure 4.3d), which fails to estimate the bridge frequency. Summary of clarity index changes shown in Table 4.3 reveals that although clarity index change of peak 3 (i.e., the closest candidate of bridge frequency peak) is significant, the change is smaller than that of peak 1, thus raising a misleading conclusion of 0.89 Hz as the bridge frequency. Possible reasons that may contribute to identification failure include driving speed fluctuations, excessive passengers movements, road irregularities, and synchronization error. Nonetheless, the resulting cross spectrum peak at the bridge frequency is relatively clear. It is possible to select peak 3 as the bridge frequency, given an a priori possible range of bridge natural frequency to exclude peak 1.

Figure 4.1 Measurement and instrumentation of vehicles

Table 4.1 Measurement cases

Case #	Driving speed v (km/h)	
	Vehicle A	Vehicle B
1	10	10
2	15	10
3	30	30
4	30	25

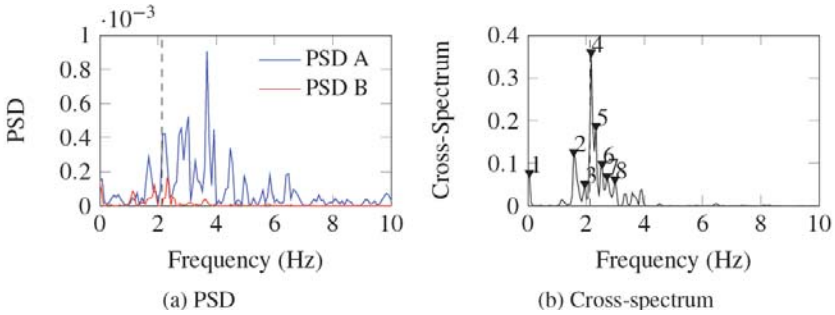

(a) PSD (b) Cross-spectrum

Figure 4.2 PSDs and Cross-spectrum from Case 2 of experiment

Table 4.2 Clarity index changes ΔI_i obtained from Case 2 of experiment

i	1	2	3	4	5	6
f_i(Hz)	0.05	1.58	1.96	2.17	2.34	2.55
$\Delta I_{i,A}$	11.57	18.81	5.95	56.60	28.47	12.84
$\Delta I_{i,B}$	13.24	18.13	1.03	49.87	18.24	9.40
Σ	24.81	36.94	6.98	106.48●	46.71	22.34

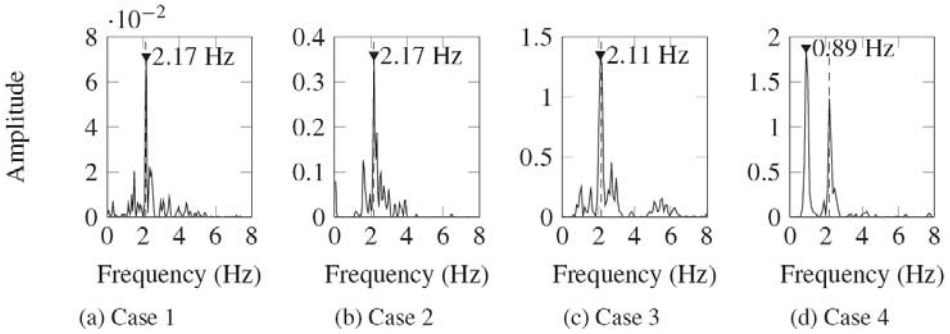

(a) Case 1 (b) Case 2 (c) Case 3 (d) Case 4

Figure 4.3 Cross-spectrum samples from various cases of experiment

Table 4.3 Clarity index changes Δl_i obtained from Case 4 of experiment

i	1	2	3	4
f_i(Hz)	0.89	1.88	2.17	2.47
$\Delta I_{i,A}$	51.12	2.86	32.60	0.65
$\Delta I_{i,B}$	44.07	1.75	34.94	8.01
Σ	95.19○	4.61	67.53	8.65

Table 4.4 Summary of measurement

	Case #			
	1	2	3	4
Success rate (%)	52.5	55.0	17.5	27.5
Estimated freq. $\hat{f}_{b,1}(Hz)$	2.18	2.17	2.20	2.24
Discrepancy $\Delta f_{b,1}{}^{*}$(%)	0.68	0.03	1.41	3.20
a^{**} (Hz)	0.02	0.02	0.07	0.07

$* \Delta f_{b,1} = \left|\hat{f}_{b,1} - f_{b,1}\right| \times 100\%;\ f_{b,1} = 2.17Hz$

**estimated by constant driving speeds of 10 km/h for Case 1 and 2; 30 km/h for Case 3 and 4

A measurement is considered as successful when the following constraint is satisfied:

$$\left|\hat{f}_{b,1} - f_{b,1}\right| \leq 0.1 f_{b,1} \tag{4.1}$$

That is, when the discrepancy between estimated natural frequency $\hat{f}_{b,1}$ and directly measured frequency $f_{b,1}$ is less than 10%. Table 4.4 presents the measurement results. The estimated frequency in the table is the average value of all identified estimations. Measurements conducted at lower speeds (Case 1 and 2) yield more accurate results compared to those conducted at higher speeds (Case 3 and 4). Note that when a priori knowledge of the natural frequency range is given, the success rates improve.

Bridge frequency peaks on vehicle response spectra typically shift by the driving speed frequency a [2, 3, 4, 6]. Thus the "apparent" bridge frequency $\hat{f}_{b,1}$ is $f_{b,1} \pm \alpha$. The estimated bridge natural frequency $f_{b,1}$ is, therefore, 2.18±0.02, 2.17±0.02, 2.20±0.07 and 2.24±0.07 Hz for Case 1, 2, 3 and 4, respectively.

5. CONCLUDING REMARKS

This paper proposes indirect estimation of the bridge natural frequency from vibration responses of two vehicles. This approach involves two vehicles moving across the bridge. The acceleration responses recorded during vehicle passage is processed to compute their individual power spectra and cross-spectrum. Through the numerical study, this approach is demonstrated to be feasible under a relatively low driving speed. Similar result is obtained from the field measurement, confirming the practicality of the strategy. The estimated bridge natural frequency is found to be in fair agreement to the values obtained from direct measurement, with the largest discrepancy of 3.20%.

ACKNOWLEDGEMENT
This research was supported by JSPS KAKENHI Grant Number 25630193.

REFERENCES

1. Salawu, O. S. (1997). Detection of structural damage through changes in frequency: a review. *Engineering structures*. **19(9):718723**.
2. Siringoringo, D. M. and Fujino, Y. (2012). Estimating bridge fundamental frequency from vibration response of instrumented passing vehicle: Analytical and experimental study. *Advances in Structural Engineering*. **15(3):417434**.
3. McGetrick P. J., Gonzalez, A, and OBrien E. J. (2009). Theoretical investigation of the use of a moving vehicle to identify bridge dynamic parameters. *Non-Destructive Testing and Condition Monitoring*. **51(8):433438**.
4. Yang, Y.-B., Lin, C. W., and Yau, J. D. (2004). Extracting bridge frequencies from the dynamic response of a passing vehicle. *Journal of Sound and Vibration*. **272(3):471493**.
5. Yang, Y.-B., Lee, Y. C., and Chang, K. C. (2014). Effect of road surface roughness on extraction of bridge frequencies by moving vehicle. *Engineering Structures*. **48:353362**.
6. Lin, C. W. and Yang, Y.-B. (2005). Use of a passing vehicle to scan the fundamental bridge frequencies: An experimental verification. *Engineering Structures*. **27(13):18651878**.
7. Yang, Y.-B., Chen, W. F., Yu, H. W., and Chan, C. S. (2013). Experimental study of a hand-drawn cart for measuring the bridge frequencies. *Engineering Structures*. **57(13):222-231**.
8. Brincker, R., Zhang, L., and Andersen, P. (2001). Modal identification of output-only systems using frequency domain decomposition. *Smart Materials and Structures*, **10: 441-445**.
9. Bendat, J. S. and Piersol A. G. (2011). Random data: analysis and measurement procedures, John Wiley Sons.
10. Yang, Y.-B., Yau, J. D., and Wu, Y. S. (2004), Vehicle-bridge interaction dynamics, World Scientific.
11. Cebon D. (1999). Handbook of vehicle-road interaction, CRC Press.
12. ISO 8608. (1995). Mechanical Vibration Road Surface Profiles Reporting of Measured Data, ISO.
13. Biggs, J. M. (1963), Introduction to structural dynamics, McGraw-Hill College.
14. Fryba L. (1999). Vibration of solids and structures under moving loads, Thomas Telford.
15. Ichikawa, S., Matsusaki, M., Tamura, H., and Tomioka, A. (2015), Development of JA-70SA MEMS accelerometer for structural health monitoring, *JAE Technical Report*. **37:9-14**